CLM - P 491

CLM - P 491

UKAEA

Preprint

TIME-RESOLVED PHOTOGRAPHY OF X-RAY EMISSION FROM CO_2 LASER GENERATED PLASMA

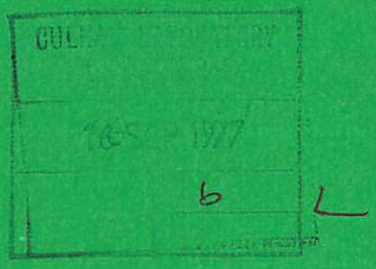

T P DONALDSON
I J SPALDING
R A WOOLLEY

CULHAM LABORATORY
Abingdon Oxfordshire

1977

This document is intended for publication in a journal or at a conference and is made available on the understanding that extracts or references will not be published prior to publication of the original, without the consent of the authors.

Enquiries about copyright and reproduction should be addressed to the Librarian, UKAEA, Culham Laboratory, Abingdon, Oxfordshire, England

CLM-P 491

TIME-RESOLVED PHOTOGRAPHY OF X-RAY EMISSION FROM CO_2 LASER GENERATED PLASMA

T.P. Donaldson*, I.J. Spalding and R.A. Woolley**

Euratom/United Kingdom Atomic Energy Authority Fusion Association,
Culham Laboratory, Abingdon, Oxon., OX14 3DB, UK.

ABSTRACT

The construction and use of an X-ray pinhole camera with a nanosecond shutter is described. Photographs of X-ray emission from plasma generated by a CO_2 laser (at incident intensities of $\lesssim 10^{13}$ Wcm^{-2}) were recorded with time and space resolution of 6 ns and $\sim$ 20 μm respectively, and the structure of localised X-ray emission regions was measured. These observations are related to contemporary theories of non-linear laser-plasma interactions.

(Submitted for publication in Optics Communications)

* Now at Institut für Angewandte Physik, Universität Bern, CH 3012, Switzerland.

** Attached from Bath University, UK.

June 1977

1. INTRODUCTION

Previous workers have normally made time-resolved measurements of X-ray emission from laser-plasmas by streak photography [1]. A method of recording X-ray framing photographs with a temporal resolution of 6 ns is described in this paper. Plasma was generated at the surface of a (semi-infinite) carbon target by a 75 J 50 ns (FWHM) multimode CO_2 laser focused by a meniscus f/4 KCl lens to intensities of up to 10^{13} Wcm^{-2} [cf 2,3]. A pinhole camera was used to photograph the resulting X-ray emission in directions parallel and perpendicular to the plasma expansion. The camera design is similar to that outlined in [4] but the space and time resolution have been improved by an order of magnitude, (see also [5]).

2. X-RAY CAMERA

The X-ray pinhole camera is shown schematically in Fig.1. X-rays are imaged by the pinhole (A) in a waveband selected by the aluminium foil (B) on to the surface of a Mullard G25-25 channel multiplier array (C). X-rays incident on the input face create photoelectrons, which are accelerated and multiplied through the array by a potential V_A of $\sim$ 1 kV. Electrons emerging from the exit face have energies of only a few tens of electron volts, and so these are collected by a second potential $V_C \sim 6$ kV applied between the exit face of the array and a 25 μm thick layer of NE 102 scintillator (D) having a decay constant of 2.4 ns. The scintillator is deposited by centrifugal evaporation of a 20% solution of xylene on to the substrate E, and is coated with 250 $\mathring{A}$ of Al to make an electrical contact. The electrons pass through the aluminium and are converted by the NE 102 to a $\lambda \sim 4500^{\circ}$A image, which is transmitted to a photographic film by the fibre-optic plate (E). Kodirex X-ray film was used because it is fast (ASA 1000) and has a linear response at optical densities up to 2.0. Good electrical contact to the faces of the array, and a vacuum better than 2×10^{-4} torr are necessary to prevent tracking; PTFE insulation was used throughout the design because of its high surface resistance and low outgassing properties.

Time resolution was achieved by gating the 1 kV acceleration voltage, V_A, across the array. V_A was derived from a spark gap, triggered by the main laser pulse. It was possible to vary both the duration of the gating pulse and the time it was applied, relative to the arrival of the main laser pulse at the target. The rise time of V_A, determined by the electrical characteristics of the channel plate, was measured to be 2 ns. The spatial resolution was calculated from the camera-target separation (system magnification $\sim$ 2), the pinhole diameter (typically $\lesssim$ 12 μm), and the 25 μm diameter of the individual channels in the array (C) to be 20 μm.

3. RESULTS AND DISCUSSION

Figs.2 and 3 were all obtained with a gating time of 6 ns and a spatial resolution of $\sim$ 20 μm. Fig.2 shows a sequence of photographs taken on successive shots with (reproducible) peak laser intensities of 10^{13} Wcm^{-2}: (a) 12 ns before, (b) 8 ns before, (c) at, (d) 4 ns after and (e) 8 ns after peak laser power. For these pictures the camera axis was normal to

the laser beam and approximately perpendicular to the plasma expansion direction, which could be adjusted by varying the position of the focal spot on the target - as shown schematically in Fig.3(a). Fig.3(b) illustrates a microdensitometer scan taken across the negative reproduced in Fig.2(b). Localised X-ray emission (having characteristic dimensions of 40 - 100 μm) is particularly noticeable in Figs.2(b) and (c), which were taken when the laser pulse was most intense. In contrast, Figs.2(d) and 2(e) show more uniform emission during the lower-intensity tail of the laser pulse. Similar X-ray pictures to Figs.2(b) and 2(c) taken almost parallel to the plasma expansion direction reveal structure of typically 40 μm. Note that emission is observed outside the (in vacuo) focal zone of the laser, due to the high thermal conductivity of the resulting plasma [6].

These results should be compared with previous time-integrated X-ray pinhole camera observations: using identical target conditions [2, 6, 7] the emission appeared (without time resolution) to be localised in filaments of ~ 100 μm diameter extending several mm in length along the laser axis. Radial structure having characteristic dimensions of 40-60 μm has also been observed by the Livermore group [8], who made time-integrated measurements of the emission from polythene and parylene foils irradiated at intensities of $\sim 8 \times 10^{13}$ Wcm^{-2} by a single-transverse-mode 1.5-3.0 ns (FWHM) CO_2 laser pulse.

The improved time and space resolution of the present measurements, which indicate transverse and longitudinal structure as small as 40 and 100 μm respectively, permits an accurate test of a recent theory of the filamentation instability [9]. This theory treats the non-linear interaction between an initially plane electromagnetic (em) wave, Stokes and anti-Stokes em waves and a density perturbation. The scattered waves grow to finite amplitude, and it is predicted that their maximum amplitude is achieved in a length of only 35-70 μm under conditions appropriate to the present experiment, in which the plasma density and temperature are typically $n_e \gtrsim 10^{18}$ cm^{-3} and Te ~ 1 keV. There is thus good quantitative agreement between theory [9] and the present time-resolved measurements. (In a preliminary outline of this work [7], comparison was made with a theory in which the scattered waves remain weak - so that filamentation

lengths between 60 and 2000 μm were predicted for densities between 9×10^{18} and 10^{18} cm^{-3}, respectively [8, 10]. It seems probable that the longer filaments seen in previous time-integrated measurements [2,8] represent the paths traced by (moving) points of emission reported here. Filamentation diameters are predicted to decrease with intensity [10], and this is well illustrated in Fig.2, where spot diameters are smallest at peak intensity. The spacing between spots, of order $10\lambda_o \sim 100$ μm, also appears to be qualitatively consistent with two-dimensional numerical simulations of strong resonance absorption and (three-dimensional) critical surface cratering [11,12]. Further work to improve the resolution of the camera is in progress; the X-ray structure will then be investigated in greater detail.

ACKNOWLEDGEMENT

I.J. Spalding thanks Dr. C.N. Lashmore-Davies for a useful discussion, and Dr. R.J. Bickerton for his interest.

REFERENCES

[1] e.g. M.H. Key, M.J. Lamb, C.L.S. Lewis and P. Sachsenmaier, Opt.Commun.19 (1976) 393.

[2] T.P. Donaldson and I.J. Spalding, Phys.Rev.Lett.36 (1976) 467.

[3] T.P. Donaldson, M. Hubbard and I.J. Spalding, Phys.Rev.Lett.37 (1976) 1348.

[4] C. Delmare, E. Laviron, M. Rabeau, D. Schirmann and G. Tonon, Acta Electronica 15 (1972) 364.

[5] M.G. Hobby, J-P. Rager and N.J. Peacock, Culham Laboratory Report CLM-R138 (1974).

[6] T.P. Donaldson, J.W. van Dijk, A.C. Elkerbout and I.J. Spalding, Proc. VII European Conf. on Controlled Fusion and Plasma Physics, CRPP Lausanne, Vol.I and II (1975) paper 82.

[7] I.J. Spalding, E. Armandillo, T.P. Donaldson, G.I. Kachen, A.C. Walker and S. Ward, 'Plasma Physics and Controlled Nuclear Fusion Research 1976', 6th Conf.Proc., Nuclear Fusion Supplement (1977), paper IAEA-CN-35/G3-3.

[8] R.A. Haas, M.J. Boyle, K.R. Manes and J.E. Swain, J.Appl.Phys.47 (1976) 1318.

[9] R. Bingham and C.N. Lashmore-Davies, Culham Laboratory Report CLM-P479 (1977).

[10] P. Kaw, G. Schmidt and T. Wilcox, Phys.Fluids 16 (1973) 1522.

[11] K. Estabrook, Phys.Fluids 19 (1976) 1733.

[12] Los Alamos Progress Report LA-6510-PR (1976) 86.

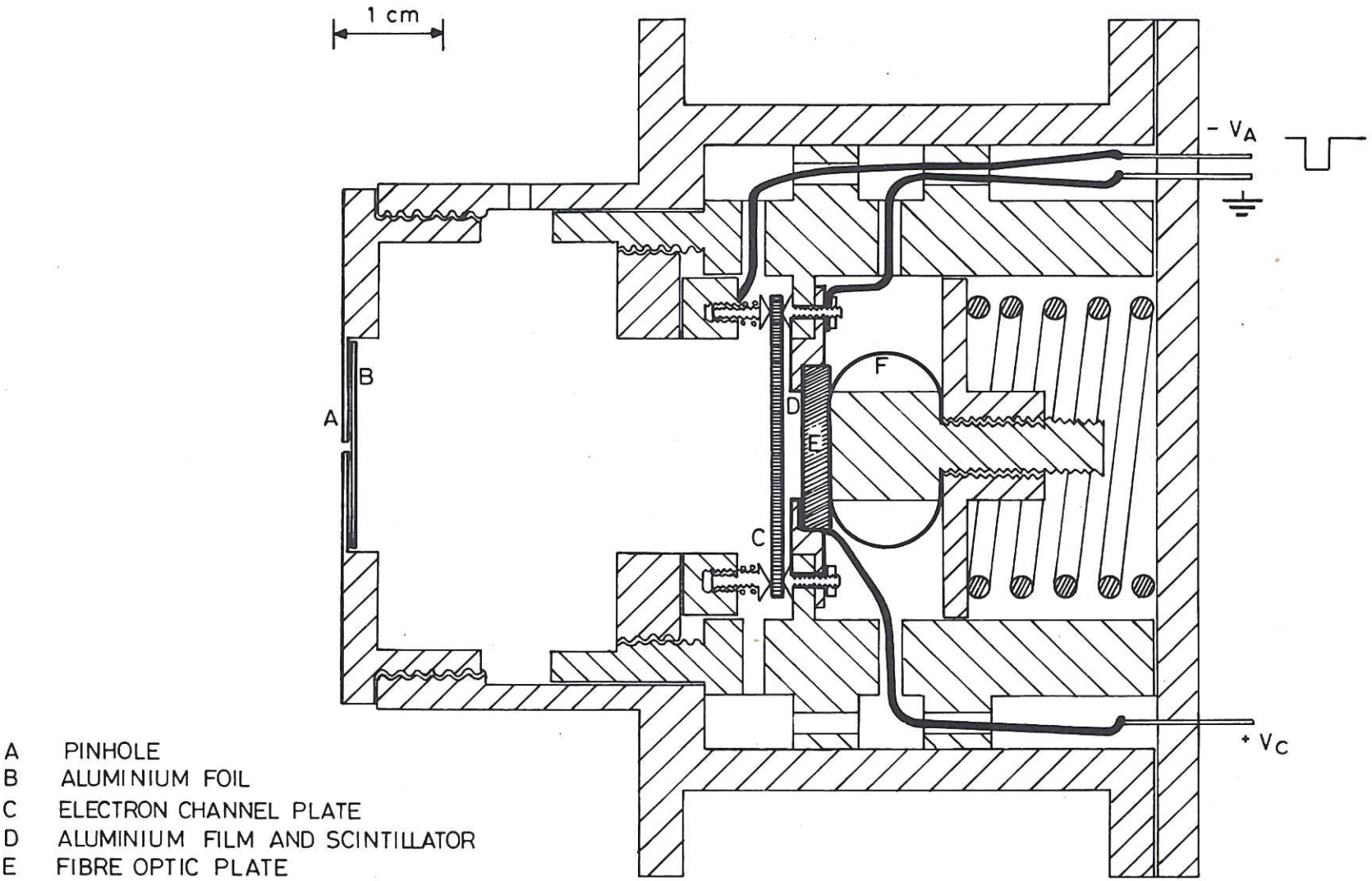

Fig.1 X-ray camera construction.

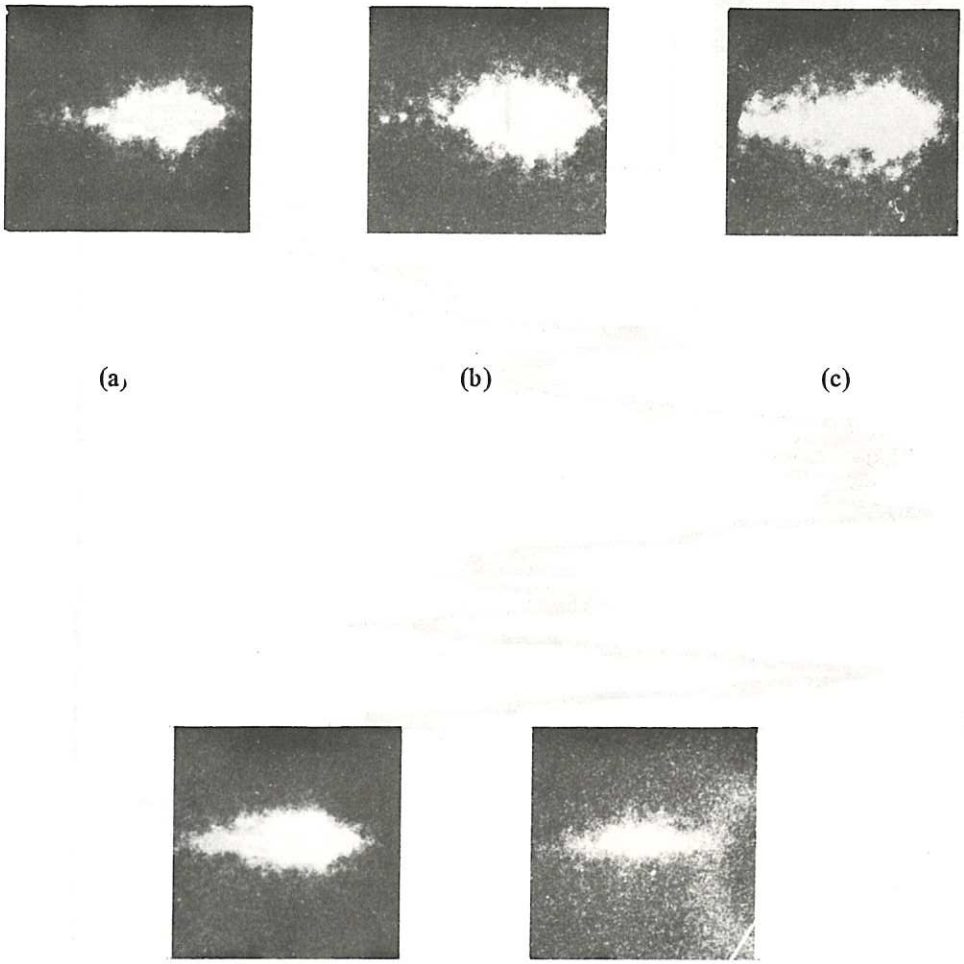

Fig.2 X-ray framing photographs taken with 6 ns exposure at time t with respect to the peak laser intensity of $\sim 10^{13}$ Wcm^{-2}. t = (a) −12, (b) −8, (c) 0, (d) +4, (e) +8 ns.

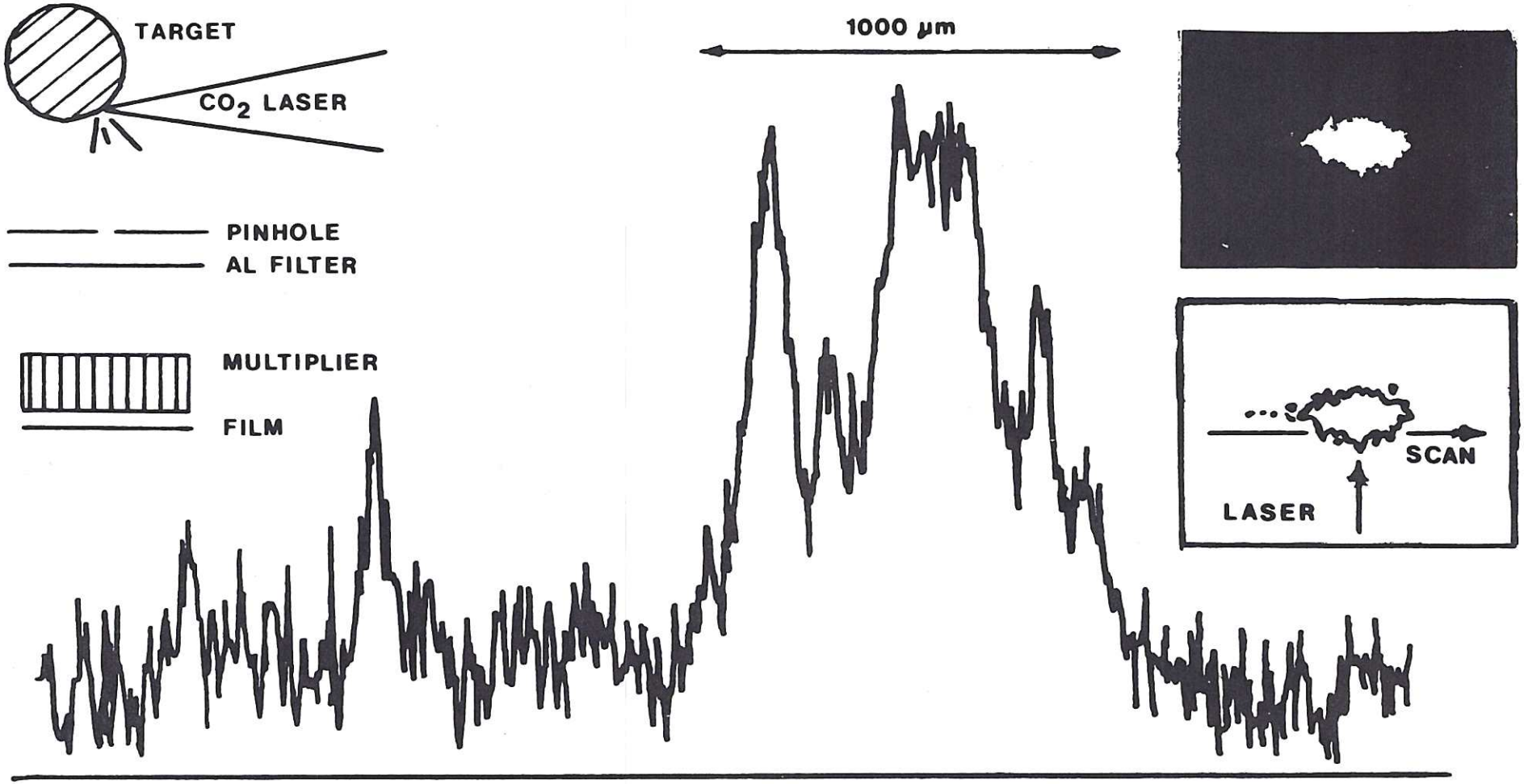

Fig.3 (a) Schematic of target geometry. (b) Microdensitometer scan across Fig.2(b), in direction indicated.